Essential role of protein kinase C ζ in transducing a motility signal induced by superoxide and a chemotactic peptide, fMLP

Kageaki Kuribayashi,[1] Kiminori Nakamura,[1,2] Maki Tanaka,[1] Tsutomu Sato,[1] Junji Kato,[1] Katsunori Sasaki,[3] Rishu Takimoto,[1] Katsuhisa Kogawa,[1] Takeshi Terui,[1] Tetsuji Takayama,[1] Takayuki Onuma,[1] Takuya Matsunaga,[1] and Yoshiro Niitsu[1]

[1]Fourth Department of Internal Medicine, [2]Department of Molecular Medicine, Sapporo Medical University School of Medicine, Chuo-ku, Sapporo 060-8543, Japan
[3]Core Facility for Therapeutic Vectors, The Institute of Medical Science, The University of Tokyo, Minato-ku, Tokyo 108-8639, Japan

Under various pathological conditions, including infection, malignancy, and autoimmune diseases, tissues are incessantly exposed to reactive oxygen species produced by infiltrating inflammatory cells. We show augmentation of motility associated with morphological changes of human squamous carcinoma SASH1 cells, human peripheral monocytes (hPMs), and murine macrophage-like cell line J774.1 by superoxide stimulation. We also disclose that motility of hPMs and J774.1 induced by a chemotactic peptide (*N*-formyl-methionyl-leucyl-phenylalanine [fMLP]) was inhibited by superoxide dismutase or *N*-acetylcystein, indicating stimulation of motility by superoxide generated by fMLP stimulation. In these cells, protein kinase C (PKC) ζ was activated to phosphorylate RhoGDI-1, which liberated RhoGTPases, leading to their activation. These events were inhibited by dominant-negative PKCζ in SASH1 cells, myristoylated PKCζ peptides in hPMs and J774.1, or a specific inhibitor of RhoGTPase in SASH1, hPMs, and J774.1. These results suggest a new approach for manipulation of inflammation as well as tumor cell invasion by targeting this novel signaling pathway.

Introduction

Under various pathological conditions, including infection, malignancy, and autoimmune diseases, tissues are incessantly exposed to reactive oxygen species (ROS) produced by infiltrating inflammatory cells. We previously disclosed that superoxide stimulated cell motility in many types of malignant cells, leading to invasion and metastasis (Yoshizaki et al., 1994; Muramatsu et al., 1995; Tanaka et al., 1997, 2001; Kogawa et al., 1999). This notion is compatible with earlier findings that superoxide generated by red blood cells from sickle cell anemia patients stimulated transendothelial migration of human myeloid leukemia, HL-60 cells, and human monocytes (Sultana et al., 1998) and that leukotriene B_4 induced transmigration of human neutrophils across epithelium, which was inhibited by intracellular ROS scavenger *N*-acetylcystein (NAC) or NADPH oxidase inhibitor diphenylene iodonium (DPI; Woo et al., 2003). Furthermore, respiratory burst (superoxide generation) and prominent motility tracking to pathogens have been known to be pivotal features of inflammatory cells, in particular, monocytes/macrophages and neutrophils, and various chemokines that stimulate inflammatory cells to generate superoxide (Bokoch, 1995; Dang et al., 2001) have been shown to simultaneously evoke chemotaxis (Thelen, 2001), suggesting a close relationship between superoxide production and motility in these cells.

Cell motility results from remodeling of acto-myosin system, which is regulated by Rho family of small GTP-binding proteins (Ridley, 2001). There is diversity in extracellular stimulants for cell migration, such as lysophophatidic acid (Moolenaar et al., 2004), platelet-derived growth factor (Chiarugi et al., 2000), and hepatocyte growth factor (Kodama et al., 2000), and many different intracellular signaling molecules that correspond to each stimulant are implicated in the activation of RhoGTPases. However, despite the fact that superoxide and chemokines are considerably important as stimulants of motility, not only from the view of tumor biology but also from the view of innate

K. Kuribayashi and K. Nakamura contributed equally to this paper.

Correspondence to Yoshiro Niitsu: niitsu@sapmed.ac.jp

Abbreviations used in this paper: DHR, dihydrorhodamine; DN, dominant-negative; DPI, diphenylene iodonium; fMLP, *N*-formyl-methionyl-leucyl-phenylalanine; hPM, human peripheral monocyte; HPX, hypoxanthine; IP, immunoprecipitation; NAC, *N*-acetylcystein; ROS, reactive oxygen species; SOD, superoxide dismutase; XOD, xanthine oxidase.

The online version of this article contains supplemental material.

The Journal of Cell Biology, Vol. 176, No. 7, March 26, 2007 1049–1060
http://www.jcb.org/cgi/doi/10.1083/jcb.200607019

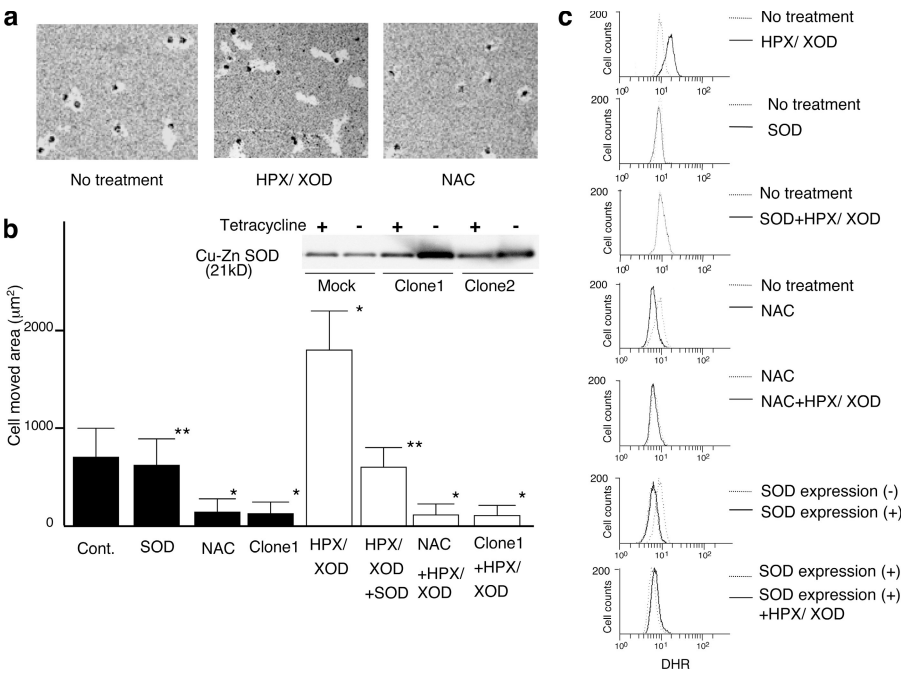

Figure 1. **Enhancement of cell motility by superoxide.** (a) On the photographs, bright areas are phagokinetic tracks where the cells moved, absorbing gold colloidal particles. (b) Areas free of gold colloidal particles of 30 individual cells were measured and shown as bar graphs. Graph shows cells with (open bars) or without (closed bars) 2 h of superoxide stimulation. Inserted figure shows immunoblotting of Cu-Zn SOD transduced SASH1 cells. SOD indicates that 100 U/ml rhCu-Zn SOD was added in the medium, NAC indicates that 40 mM NAC was added in the medium, and clone 1 indicates SASH1 cells that were transfected with Cu-Zn SOD expression vector. *, $P < 0.01$, compared with the value without any treatment; **, $P > 0.05$, compared with the value without any treatment. Error bars indicate SEM. (c) SASH1 cells were treated as described in the figure, and intracellular ROS level was monitored by DHR as fluorescent probe. NAC indicates that 40 mM NAC was added in the medium 20 min before the assay, SOD expression (−) indicates Cu-Zn SOD transfectant without Cu-Zn SOD expression by adding tetracycline in the medium, and SOD expression (+) indicates SOD transfectant with Cu-Zn SOD overexpression by removing tetracycline from the medium.

immunity, no detailed exploration on the motility relevant to these stimulants has been performed to date.

In the present study, we first reveal that, in human squamous carcinoma SASH1 cells, superoxide activates PKCζ, which phosphorylates RhoGDI-1, in turn liberating RhoGTPases from RhoGDI-1, leading to their activation. Then, using human peripheral monocytes (hPMs) and murine macrophage-like cell line J774.1, we examined whether the superoxide extracellularly generated by hypoxanthine/xanthine oxidase (HPX/XOD), or which they themselves produced upon treatment with a chemotactic peptide, *N*-formyl-methionyl-leucyl-phenylalanine (fMLP), stimulated their motility, and found that both extracellularly generated and self-produced superoxide augmented their motility. Furthermore, we confirmed that the PKCζ–RhoGDI-1 phosphorylation–RhoGTPases activation signaling pathway was also involved in the motility of hPMs and J774.1 stimulated with superoxide or fMLP.

Results

Relevance of superoxide to motility of SASH1 cells

To examine the effect of superoxide on cell motility for SASH1 cells, we performed a phagokinetic track assay (Fig. 1, a and b). The cells without any treatment showed some movement (intrinsic motility), which was not affected by the addition of Cu-Zn superoxide dismutase (SOD). When the cells were treated with HPX/XOD, the motility was enhanced as compared with that of nontreated cells. The enhancement of cell motility by superoxide stimulation was canceled with the addition of Cu-Zn SOD, indicating that superoxide by itself, not other types of ROS, is the factor that enhances the cell motility. Treatment of the cells with NAC resulted in almost complete suppression of intrinsic motility to the basal level, suggesting that endogenous ROS is affecting their motility. This effect of endogenous ROS on motility was not seen in Cu-Zn SOD transfectant (clone 1), suggesting that the endogenous ROS responsible for the cell motility is mainly superoxide. Incidentally, the suppressive effects observed in the other Cu-Zn SOD clones, including clone 2, were essentially the same as those seen in clone 1 (unpublished data). We also performed migration a assay. Cells treated with HPX/XOD showed higher motility than nontreated cells, and it was blocked by the addition of Cu-Zn SOD (Fig. S1 a, available at http://www.jcb.org/cgi/content/full/jcb.200607019/DC1).

To confirm that the motility of SASH1 cells is related to their intracellular ROS level, we analyzed dihydrorhodamine (DHR) 123 staining of SASH1 cells by FACS (Fig. 1 c). The nontreated SASH1 cells showed some staining intensity (endogenous ROS), which was not suppressed by extracellularly added Cu-Zn SOD. This staining intensity was clearly enhanced by treatment with superoxide. NAC pretreatment or Cu-Zn SOD overexpression suppressed the intensity to the basal levels and maintained the basal intensity even after superoxide treatment. Incidentally, extracellular superoxide was not detectable with this cell line measured by cytochrome *c* method (unpublished data), indicating that the cells were not releasing superoxide extracellularly. These results suggest the relevance of superoxide to motility of SASH1 cells.

Superoxide reorganizes actin structure and activates Rho family GTPases in SASH1 cells

To investigate the mechanism of enhancement of cell motility by superoxide, we first examined the morphological changes in SASH1 cells (Fig. 2 a). The parental cells had a rather round shape with small lamellipodia. In the parental cell stimulated

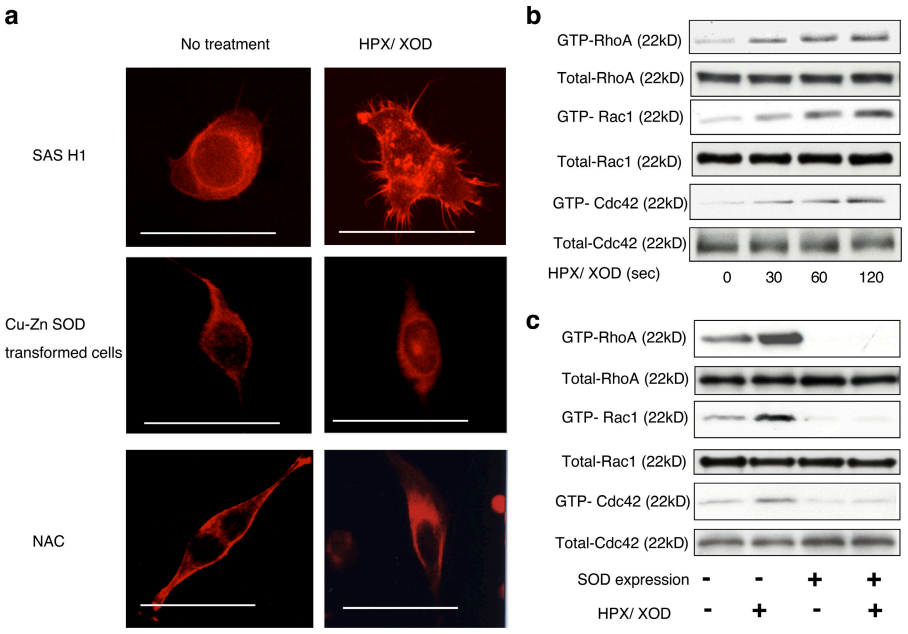

Figure 2. **Activation of Rho family GTPases by superoxide.** (a) F-actin staining of SASH1 cells, Cu-Zn SOD transfectants, and SASH1 cells with 40 mM NAC pretreatment. Confocal images of cells with or without 5 min of superoxide stimulation are shown. Bars, 50 μm. (b) RhoGTPases activity of SASH1 cells with or without superoxide stimulation was analyzed by pull-down assay. (c) RhoGTPase activity of Cu-Zn SOD transfectants with or without superoxide was analyzed by pull-down assay.

with superoxide, there was increment of F-actin and a more discrete formation of lamellipodia and filopodia than in that without stimulation. Cu-Zn SOD transduced clone 1 showed less actin staining with spindle-shaped morphology (dendrite-like formation). Similar morphological features were observed with NAC-treated cells. This spindle-shaped morphology was unchanged even after superoxide stimulation.

When we analyzed the activity of Rho family of small GTPases (Rho, Rac, and Cdc42) by pull-down assay, some activated forms of these proteins were identified in parental cells, and the superoxide stimulation apparently enhanced these proteins (Fig. 2 b). This activation of Rho family GTPases was markedly inhibited by overexpression of Cu-Zn SOD (Fig. 2 c). The results of the pull-down assay were verified by analyzing the proteins relocalizing to the plasma membrane (Fig. S2, available at http://www.jcb.org/cgi/content/full/jcb.200607019/DC1). RhoA, Rac1, and Cdc42 each showed an apparent membrane translocation followed by spontaneous detachment from the membrane in a relatively short time after superoxide treatment; however, the detachment of Rac1was somewhat retarded compared with the other two GTPases.

Effects of inhibitors of Rho, Rac, and Cdc42 on the motility and morphological change relevant to superoxide in SASH1 cells

To verify the involvement of Rho, Rac, and Cdc42 in motility and morphological changes relevant to superoxide, we examined the effect of specific inhibitors of the proteins on these cellular events in SASH1 cells. Treatment with C3 substantially suppressed the motility of SASH1 cells down to the basal levels, equivalent to that of NAC-pretreated cells, irrespective of superoxide stimulation.

Transfectants of dominant-negative (DN) Cdc42 (DNCdc42) and Rac1 (DNRac1), exhibited impaired motility similar to that of C3-treated cells treated with or without superoxide (Fig. 3 a). When the morphology of SASH1 cells was examined, treatment with C3 resulted in a slight reduction of F-actin intensity (Fig. 3 d) compared with that of nontreated cells (Fig. 3 b) and showed new dendrite-like formations and multiple nuclei in a

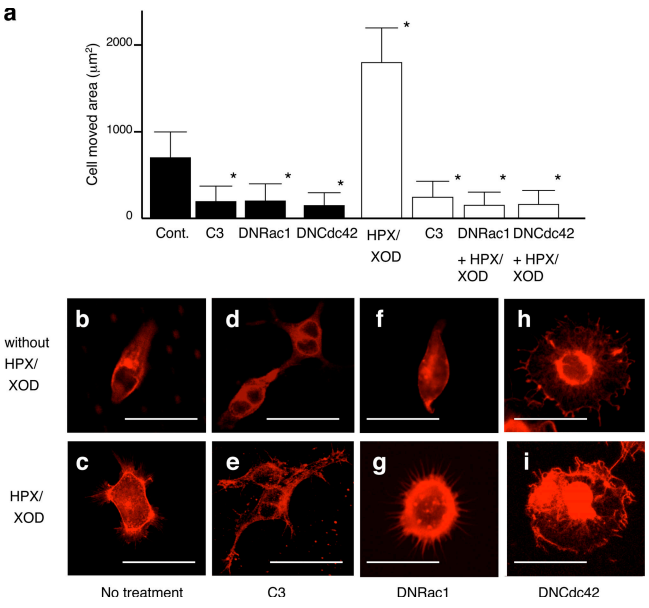

Figure 3. **Effect of inhibiting RhoGTPase activity on superoxide-induced cell motility and morphological change.** (a) Phagokinetic track assay of SASH1 cells. Cont indicates SASH1 cells, C3 indicates SASH1 cells pretreated with 100 μg/ml C3 for 48 h, DNRac1 indicates DNRac1 transduced SASH1 cells, and DNCdc42 indicates DNCdc42 transduced SASH1 cells. After 2 h with (open bars) or without (closed bars) superoxide stimulation, cell-moved areas were measured and shown as bar graphs. *, $P < 0.01$, compared with the value without any treatment. Error bars indicate SEM. (b–i) F-actin staining of the cells with or without 5 min of superoxide treatment. (b and c) SASH1 cells; (d and e) SASH1 cells pretreated with 100 μg/ml C3 for 48 h; (f and g) DNRac1 transduced SASH1 cells; (h and i) DNCdc42 transduced SASH1 cell. Bars, 50 μm.

single cell caused by inhibition of cytoplasmic division. In these cells, superoxide treatment did not increase F-actin intensity, but apparently induced lamellipodia or filopodia formation (Fig. 3 e). DNRac1 transfectant was not substantially different from the parental cells without the stimulation (Fig. 3 f), whereas superoxide treatment of the cells induced F-actin increment and filopodia formation, although lamellipodia formation was not observed (Fig. 3 g). Transduction of DNCdc42 caused loss of cell polarity with relatively concentrated F-actin staining in the center of the cell (Fig. 3 h). The morphological characters of DNCdc42 became more apparent by treatment with superoxide (Fig. 3 i). These results are compatible with the previous notion that F-actin is regulated by Rho; that activation of Rac1 is associated with lamellipodia formation (Nobes and Hall, 1995), although it does not associate much with F-actin or filopodia formation; and that Cdc42 regulates cell polarity and filopodia (Etienne-Manneville, 2004).

Superoxide activates RhoGTPases via phosphorylation of RhoGDI-1 by PKCζ in SASH1 cells

As evidence that shows the relationship between PKC and RhoGTPases is accumulating (Hall, 1994; Balboa and Insel, 1995; Machesky and Hall, 1996; Laudanna et al., 1998; Uberall et al., 1999; Coghlan et al., 2000; Mehta et al., 2001; Slater et al., 2001), we examined the possibility that PKC is a molecule that links superoxide with Rho family GTPases. The PKC inhibitor, calphostin C, dose-dependently inhibited cell motility (Fig. 4 a) as well as the activity of Rho family GTPases (Fig. 4 b) in superoxide-treated or nontreated SASH1 cells (Fig. 4, a and b). At 500 nM calphostin C, cell motility was suppressed to basal level and almost complete inhibition of the RhoGTPase activity was attained. The results suggested that PKC may be an upstream molecule of RhoGTPases and that it regulates cell motility stimulated by superoxide.

To determine which isozyme of PKC is responsible for the Rho family activation, we studied PKC isozymes that were expressed in SASH1 cells by immunoblotting and seven PKC isozymes, PKCα, -β, -γ, -δ, -ε, -μ, and -ζ, were found to be expressed (Fig. 4 c, lane 1). As members of the Rho family of small GTPases form complexes with RhoGDI-1 in cytosol in their resting state and the first step of Rho family activation is their liberation from RhoGDI-1 (Ueda et al., 1990; Isomura et al., 1991; Chuang, et al., 1993; Hancock and Hall, 1993; Hart et al., 1998), we next identified the PKC isozyme that interacted with RhoGDI-1–RhoGTPases by pull-down assay using the anti–RhoGDI-1 antibody. As shown in Fig. 4 c, among seven isozymes expressed in SASH1 cells, only PKCζ was detected in the immunoprecipitates, and the association was enhanced by superoxide treatment. Furthermore, this coprecipitation of PKCζ with RhoGDI-1 was clearly inhibited in NAC-pretreated (Fig. 4 e) or Cu-Zn SOD transduced cells (Fig. 4 f), indicating dependency of PKCζ activation on superoxide stimulation. We then examined whether PKCζ kinase activity is stimulated in

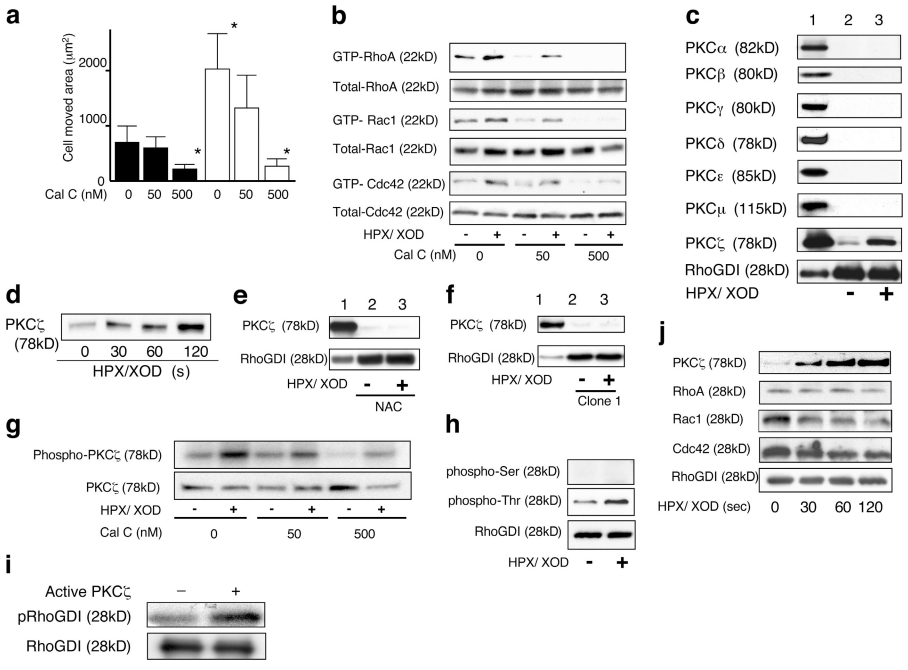

Figure 4. **Superoxide induces RhoGDI phosphorylation by PKCζ, leading to RhoGTPase liberation from RhoGDI.** (a) After SASH1 cells were treated with calphostin C for 15 min, they were stimulated with (open bars) or without (closed bars) superoxide for 2 h. Cell motility was measured and shown in the bar graph. *, $P < 0.01$, compared with the value without any treatment. Error bars indicate SEM. (b) After 15 min of pretreatment of calphostin C, SASH1 cells were treated with or without superoxide for 2 min, and RhoGTPase activity was measured by pull-down assay. (c, e, and f) SASH1 cells were treated with or without superoxide, lysed, and subjected to IP using anti-RhoGDI antibody. The samples were then electrophoresed and immunoblotted by the antibodies indicated in the figures. Lane 1, positive controls; lane 2, without superoxide treatment; lane 3, 2 min of superoxide treatment. (c) SASH1 cells; (e) SASH1 cells pretreated with 40 mM NAC for 20 min; (f) Cu-Zn SOD overexpressed SASH1 cells (clone 1). (d) Translocation assay of PKCζ in SASH1 cells treated with superoxide. 4×10^7 cells were treated with superoxide for the indicated times and subjected to subcellular fractionation. Plasma membrane fractions were electrophoresed and immunoblotted by the antibody indicated in the figure. (g) Activity of PKCζ was measured by its phosphorylation state as described in Materials and methods. SASH1 cells were pretreated by calphostin C of the concentrations indicated in the figure. (top) Phosphorylated PKCζ confirmed by autoradiography; (bottom) immunoblotting of PKCζ to confirm that an equal amount of the protein was loaded. (h) Superoxide phosphorylates threonine residue of RhoGDI. SASH1 cells with or without 2 min of superoxide stimulation were lysed and immunoprecipitated with anti-RhoGDI antibody. Immunoprecipitates were electrophoresed and immunoblotted by antibodies indicated in the figure. (i) Recombinant active PKCζ phosphorylated RhoGDI-1 immunoprecipitated from SASH1 cell lysate. In vitro kinase assay was performed as described in Materials and methods. (top) [^{32}P]RhoGDI-1; (bottom) RhoGDI-1 immunoblotting. (j) PKCζ associated with and RhoGTPases dissociated from RhoGDI after superoxide stimulation. SASH1 cells with or without superoxide treatment were subjected to IP by anti-RhoGDI antibody, and the samples were immunoblotted by the antibodies indicated in the figure.

superoxide-treated cells. As shown in Fig. 4 g, phosphorylated PKCζ was increased in superoxide- treated cells as compared with nontreated cells revealed by in vitro phosphorylation assay. The PKCζ activity was suppressed by calphostin C in a dose-dependent manner as described previously (Xu and Clark, 1997; Furukawa et al., 1999; Fitzgerald et al., 2000; Liu et al., 2000). Further, PKCζ activation was confirmed by its translocation to the plasma membrane (Fig. 4 d). The PKCζ molecule consists of two functional domains, reportedly, a regulatory N-terminal domain and a catalytic C-terminal domain (Spitaler and Cantrell, 2004). We investigated which domain interacts with RhoGDI-1 in superoxide-treated SASH1 cells by pull-down assay. As shown in Fig. S3 a (available at http://www.jcb.org/cgi/conent/full/jcb.200607019/DC1), RhoGDI-1 did associate with the C-terminal catalytic domain but not with the N-terminal regulatory domain. The fact that PKC is a member of serine-threonine kinases, and RhoGDI-1's interaction with the catalytic domain of PKCζ, prompted us to examine the possibility of phosphorylation of RhoGDI-1 by PKCζ. Immunoprecipitates with anti–RhoGDI-1 antibody were found to contain threonine but not serine-phosphorylated RhoGDI-1 in both superoxide-treated and nontreated cells, though in the latter the threonine-phosphorylated RhoGDI-1 increased more than in the former (Fig. 4 h).

To further elucidate whether PKCζ directly phosphorylate RhoGDI-1 upon superoxide stimulation or, rather, activates a putative kinase, which in turn phosphorylates RhoGDI-1, RhoGDI-1 was purified from SASH1 cell lysate by immunoprecipitation (IP) and incubated with recombinant active PKCζ. As shown in Fig. 4 i, the intensity of the band representing [^{32}P]RhoGDI-1 in the PKCζ-treated preparation was apparently increased compared with that in the nontreated preparation, indicating the direct action of PKCζ on RhoGDI-1.

On the other hand, when recombinant RhoGDI-1 was simply incubated with recombinant active PKCζ, phosphorylation of RhoGDI-1 was undetectable (unpublished data). Therefore, it is highly conceivable that some cofactors that coprecipitated with RhoGDI from the cell lysate were required for RhoGDI-1 phosphorylation by PKCζ. The small RhoGTPase family proteins are potential cofactors. Upon superoxide stimulation, PKCζ interacts with RhoGDI-1/small RhoGTPase family protein complex; binding of PKCζ to the complex stimulates the release of the small RhoGTPases from RhoGDI (Fig. 4 j). Incidentally, weak but nonnegligible phosphorylation of RhoGDI-1 observed in the PKCζ-nontreated preparation (Fig. 4 i, left) may be ascribed to the activity of endogenous PKCζ that has been coprecipitated with RhoGDI-1.

It is plausible that there is a kinase that phosphorylates RhoGDI downstream of PKCζ. To test this, recombinant active PKCζ was incubated with cell lysate to activate the putative kinase. PKCζ was subsequently removed by IP, and recombinant GST–RhoGDI-1 was incubated with the lysate but was not phosphorylated by the PKCζ-deficient cell lysate (Fig. S3 b). The results denied the possibility of the other kinase downstream of PKCζ.

We then extended our investigation to examine the kinetics of complex formation of RhoGDI-1 and Rho family GTPases or PKCζ by IP using anti–RhoGDI-1 antibody. An immunoreactive band of PKCζ increased in intensity from 30 s until 2 min after superoxide treatment (Fig. 4 j). However, in the same time course, RhoGDI-1 showed no appreciable changes, whereas the bands of all Rho family GTPases showed gradual decrement, indicating the dissociation of RhoGTPases from the complex and their eventual activation upon initiation of superoxide stimulation. These dissociation and association phenomena were not obvious in DNPKCζ transduced cells (Fig. 5 e).

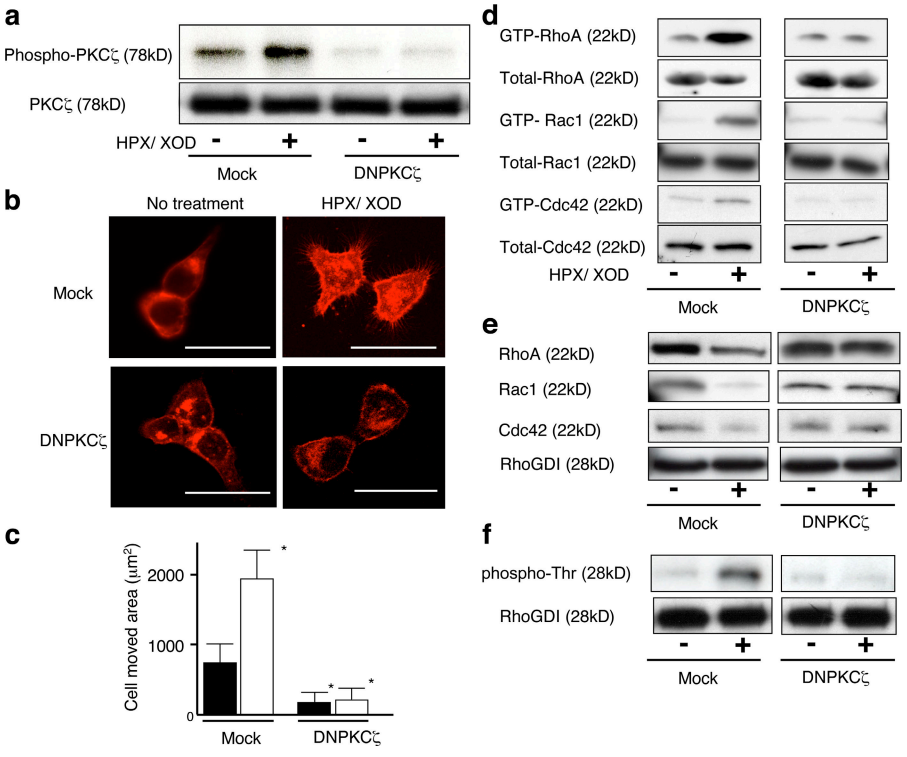

Figure 5. **DNPKCζ inhibits superoxide-induced cell motility and Rho family GTPase activation.** (a) PKCζ activity of mock and DNPKCζ transfectants. (top) Autoradiography of phosphorylated PKCζ; (bottom) Immunoblotting of PKCζ. (b) After mock and DNPKCζ transfectants were stimulated with or without superoxide for 5 min, they were subjected to F-actin staining. Bars, 50 μm. (c) Motility of mock and DNPKCζ transfectants was studied and is shown in the bar graph. Cells without superoxide stimulation are indicated with closed bars, and cells with superoxide stimulation are indicated with open bars. *, $P < 0.01$, compared with the value without any treatment. Error bars indicate SEM. (d) Mock and DNPKCζ transfectants were stimulated with or without superoxide for 2 min, and RhoGTPase activity was studied by pull-down assay. (e and f) Mock and DNPKCζ transfectants were subjected to IP by anti-RhoGDI antibody, and the samples were immunoblotted with the antibodies indicated in the figure.

DNPKCζ inhibits superoxide-induced morphological change, Rho family GTPase activation, and motility of SASH1 cells

To further validate the implication of PKCζ in morphological changes, Rho family activation, and cell motility induced by superoxide, SASH1 cells were transfected with DNPKCζ plasmid to suppress PKCζ activity. We first confirmed that the transfectants expressed the DNPKCζ protein (unpublished data) and that DNPKCζ was truly active to inhibit autophosphorylation of PKCζ in vitro (Fig. 5 a). This DNPKCζ transfectant showed morphological features that were similar to those of the parental cells (Fig. 5 b), and these features were not apparently affected by superoxide treatment. Moreover, activation of Rho family proteins with superoxide stimulation was not seen in the DNPKCζ transfectants (Fig. 5 d). Furthermore, intrinsic cell motility or cell motility induced by superoxide was also impaired in the transfectant (Fig. 5 c). In the transfectant of DNPKCζ, the associations of RhoA, Rac1, and Cdc42 with RhoGDI were not affected (Fig. 5 e) and showed no increase of threonine phosphorylation of RhoGDI even after HPX/XOD treatment (Fig. 5 e). These results indicate that the activation of Rho family, the changes of cell morphology, and stimulation of cell motility relevant to superoxide were evoked by PKCζ.

Motility of J774.1 murine macrophage-like cell line is induced by superoxide through activation of PKCζ and RhoGTPases

These observations led us to speculate that superoxide may be actively involved in the motility of inflammatory cells as well, most likely via an autocrine mechanism, as they are known to exhibit prominent motility and generate superoxide by themselves. We validated this speculation by using macrophage-like cell line J774.1. As shown in Fig. 6 a, certain amount of superoxide was detected in the medium of the cells and their motility was significantly suppressed by addition of Cu-Zn SOD to the medium (Fig. 6 b), indicating autocrine stimulation of cell motility by superoxide released from the cells themselves (automotility). When the cells were treated with NAC, their motility (both auto and intrinsic) was almost completely suppressed (Fig. 6 b), indicating that not only automotility but also intrinsic motility is mediated by ROS inside the cells. Enhancement of the motility was clearly observed with the cells treated with superoxide. This enhanced motility was blocked by the addition of Cu-Zn SOD to the level of the cells treated with Cu-Zn SOD alone and to the basal level by NAC, suggesting that the effect of extracellularly added superoxide is also operating intracellularly as ROS. These results were compatible with the morphological findings (Fig. 6 c). When nontreated cells are compared with NAC-treated cells, which resemble Cu-Zn SOD transfected SASH1 cells, F-actin increment, small but apparent formation of filopodia, and little lamellipodia were seen, supporting the speculation of autoactivation of cells by self-produced superoxide. The F-actin intensity, filopodia, and lamellipodia formation seen in nontreated J774.1 cells were further enhanced in superoxide-treated cells.

To confirm the involvement of RhoGTPases in the superoxide-relevant motility of J774.1 cells, we conducted a pull-down assay for these enzymes. As shown in Fig. 6 d, superoxide activated RhoA, Rac1, and Cdc42 in a time-dependent manner.

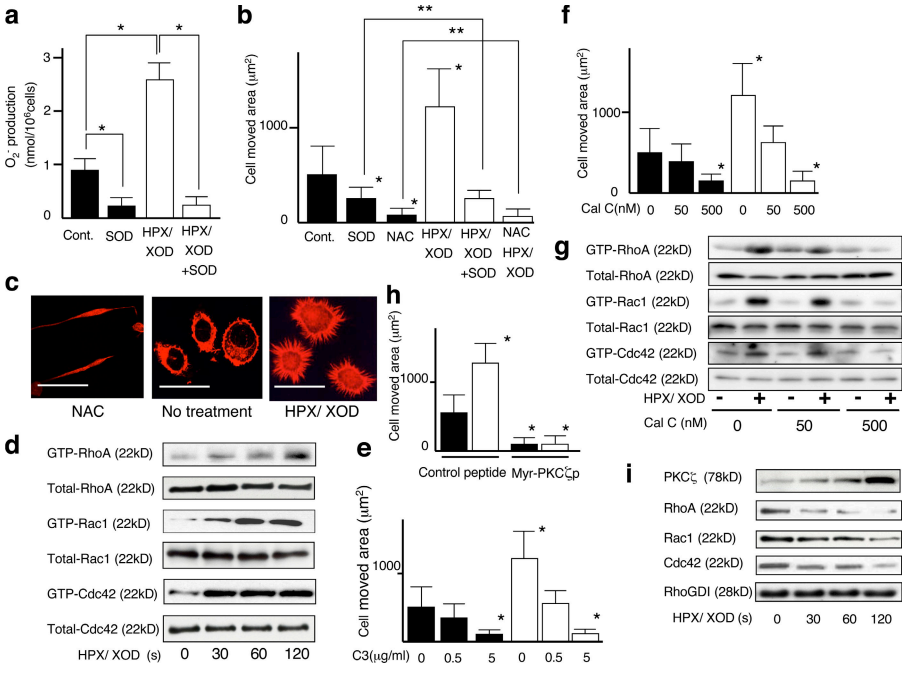

Figure 6. **Superoxide stimulates motility through sequential activation of PKCζ, phosphorylation of RhoGDI, and RhoGTPases in J774.1 murine macrophage-like cell line.** (a) The amount of superoxide produced by J774.1 cells was measured by cytochrome *c* method. Cells with (open bars) or without (closed bars) 2 min of superoxide treatment are shown. SOD indicates that 100 U/ml rhCu-Zn SOD was added in the medium. *, $P < 0.01$. (b, e, f, and h) Motility of J774.1 cells with or without 2 h of superoxide stimulation. NAC indicates that 40 mM NAC was added in the medium. C3 indicates that the cells were pretreated with the indicated concentrations of C3 for 48 h. Cal C indicates that the cells were pretreated with the indicated concentrations of calphostin C for 15 min. (h) The cells are pretreated with either 50 μM control peptide or 50 μM myr-PKCζp for 30 min *, $P < 0.01$, compared with the value without any treatment; **, $P > 0.05$. (c) F-actin staining of J774.1 cells with or without superoxide stimulation. Bars, 20 μm. (d) After the indicated times of superoxide treatment, RhoGTPase activity of J774.1 cells was studied by pull-down assay. (g) J774.1 cells were pretreated with calphostin C of the concentrations indicated in the figure and stimulated with or without 2 min of superoxide, and RhoGTPase activity was studied. (i) J774.1 cells with the indicated times of superoxide treatment were subjected to IP using anti-RhoGDI antibody and immunoblotted with the antibodies indicated in the figure. Error bars indicate SEM.

Then, to evaluate whether the activation of these GTPases is associated with cell motility, we intended to examine the motility of the cells treated with specific inhibitors for RhoA, Rac1, and Cdc42. However, transduction of DN RhoGTPases was not feasible in this cell line; therefore, only C3 treatment was performed. As shown in Fig. 6 e, treatment with C3 at a concentration of 5 μg/ml caused suppression of motility of both superoxide-treated and nontreated J774.1 cells to the basal levels, suggesting the dependency of the motility on Rho. We next studied whether there is PKCζ involvement in this signaling pathway. Among PKCα, -β, -γ, -δ, -ε, -μ, and -ζ, only PKCζ associated with RhoGDI-1 examined by pull-down assay using RhoGDI-1 antibody (unpublished data). To confirm the role of PKCζ in cell motility and RhoGTPase activation, J774.1 cells were treated with calphostin C. Both cell motility (Fig. 6 f) and RhoGTPase activation (Fig. 6 g) of superoxide-treated and nontreated cells were substantially suppressed to basal levels by 500 nM calphostin C. We used myristoylated pseudosubstrate peptide of PKCζ (myr-PKCζp) to inhibit the enzyme activity. Motility of J774.1 cells with or without superoxide stimulation was impaired by myr-PKCζp compared with control peptide–treated cells (Fig. 6 h). The phenomena of association of PKCζ and dissociation of GTPases from the RhoGDI-1–GTPases complex upon superoxide stimulation found in SASH1 cells were also confirmed in this cell line (Fig. 6 i), and dissociation and association were inhibited by calphostin C (not depicted). As shown in Fig. S4 (available at http://www.jcb.org/cgi/content/full/jcb.200607019/DC1), Rac2 was also activated by superoxide in J774.1 cells.

Motility of human peripheral blood monocytes is induced by superoxide through PKCζ–RhoGDI-1–RhoGTPases signal

We further extended our study by examining human monocytes collected from the peripheral blood of a healthy volunteer. As shown in Fig. S5 a (available at http://www.jcb.org/cgi/content/full/jcb.200607019/DC1), addition of Cu-Zn SOD significantly lowered the motility of hPMs, indicating autocrine activation of motility by superoxide, which they generated (automotility). Treatment with NAC almost completely suppressed their motility, a finding consistent with that observed with J774.1. Augmentation of motility by superoxide treatment was also observed with hPMs (Fig. S5 a), as was the case with SASH1 and J774.1, and the motility was positively related with superoxide production (Fig. S5 b). Morphologically, NAC-treated hPMs showed spindle form with dendrite formation, whereas nontreated cells exhibited a rather round shape with slightly increased F-actin staining and formation of some small filopodia (Fig. S5 c). Such F-actin staining or filopodia formation of hPMs was further strengthened by treatment with superoxide (Fig. S5 c). As shown in Fig. S5 d, the activation of RhoGTPases by superoxide was also confirmed. Moreover, movement of hPMs treated with or without superoxide was strongly suppressed by C3 to the basal levels (Fig. S5 e). To investigate whether PKCζ is also involved in the motility of hPMs, we pulled down the isozyme with anti–RhoGDI-1 antibody in the cells treated with or without superoxide. Coprecipitation of PKCζ with RhoGDI-1 was clearly observed in cells treated with superoxide and seen with less intensity in those without superoxide (Fig. 7 a). RhoGDI-1 was apparently phosphorylated, as revealed by immunoblotting using anti-phosphothreonine antibody in both superoxide-treated and nontreated hPMs, with much higher intensity in the former than the latter (Fig. 7 a). As shown in Fig. 7 b, PKCζ kinase activity was increased by superoxide stimulation. To examine the involvement of PKCζ in the motility of hPMs, the cells were treated with myr-PKCζp. As shown in Fig. 7 c, motility of both superoxide-stimulated and nonstimulated cells were almost completely suppressed to basal level by myr-PKCζp. The activation of RhoGTPases in hPMs was also clearly suppressed by treatment with myr-PKCζp (Fig. 7 d). Association of

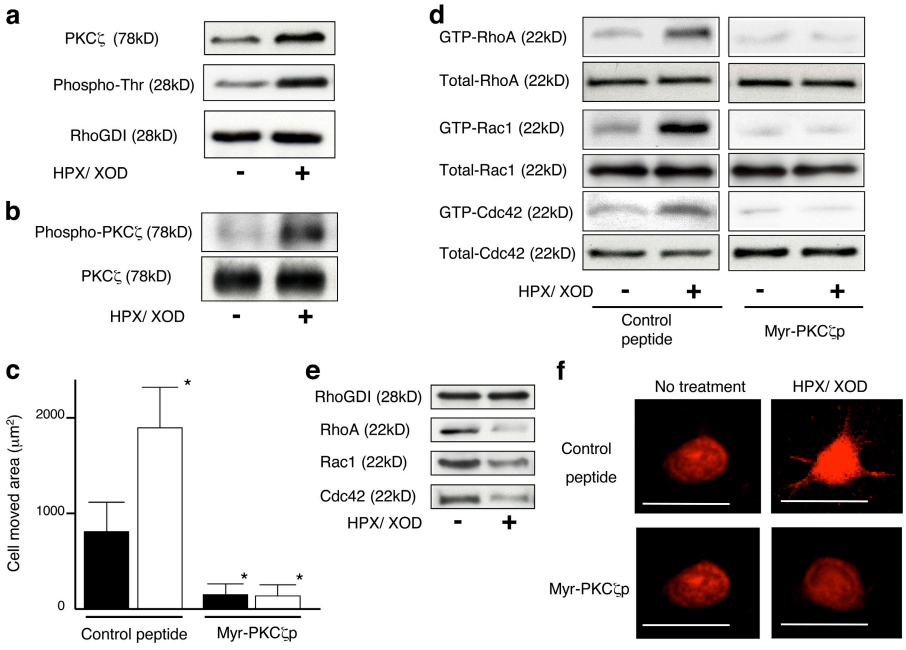

Figure 7. **Superoxide stimulates motility through sequential activation of PKCζ, phosphorylation of RhoGDI, and activation of RhoGTPases in hPMs.** (a) hPMs with or without 2 min of superoxide stimulation were subjected to IP using anti-RhoGDI antibody and immunoblotted with the antibodies indicated in the figure. (b) PKCζ activity of hPMs before and after 2 min of superoxide stimulation. (top) Autoradiography; (bottom) immunoblotting. (c) Phagokinetic track assay of hPMs stimulated with (open bars) or without (closed bars) superoxide for 2 h. The cells were pretreated with 50 μM myr-PKCζp or control peptide for 30 min before the assay. *, $P < 0.01$, compared with the value without superoxide stimulation. Error bars indicate SEM. (d) hPMs were pretreated with 50 μM of the indicated peptides, and RhoGTPase activity with or without 2 min of superoxide stimulation was studied. (e) hPMs were subjected to IP using anti-RhoGDI antibody and immunoblotted with the antibodies indicated in the figure. (f) F-actin staining of hPMs pretreated with 50 μM myr-PKCζp or control peptide. Bars, 20 μm.

PKCζ with RhoGDI-1 upon superoxide stimulation and dissociation of RhoGTPases from RhoGDI-1 were confirmed with hPMs as well (Fig. 7 e). The effect of myr-PKCζp on the morphology of hPMs was further examined (Fig. 7 f). hPMs had a round shape with small filopodia and mild F-actin staining. Filopodia formation and F-actin staining were enhanced, and lamellipodia formation became evident by treatment with superoxide. In myr-PKCζp–treated cells, filopodia and lamellipodia formation were hardly seen and intensity of F-actin was rather weak compared with nontreated cells. The association of PKCζ with and dissociation of RhoGTPases from RhoGDI-1 were impaired in myr-PKCζ–treated cells (unpublished data).

Response of J774.1 cells and hPMs to fMLP

To investigate the role of superoxide in the motility of monocytes/macrophages that are stimulated by chemokine, we examined the superoxide generation (Fig. 8 a and Fig. S5 f) and motility (Fig. 8 b and Fig. S5 g) of J774.1 cells (Fig. 8) and hPMs (Fig. S5, f and g) treated with fMLP. fMLP treatment substantially stimulated superoxide production by these cells (Fig. 8 a and Fig. S5 f). The motility of these cells treated with fMLP was significantly increased, and this increment was negated by the addition of Cu-Zn SOD, NAC, or DPI (Fig. 8 b and Fig. S5 g), indicating that the motility of these cells is prompted by superoxide generated by themselves through activated NADPH oxidase in an autocrine manner. When fMLP-treated cells were treated with myr-PKCζp, the motility of the cells was totally suppressed to basal levels. Essentially the same results were obtained by migration assay (Fig. S1 b). Thus, it was suggested that PKCζ is directly activated by fMLP, which utilizes the same PKCζ–RhoGDI-1–GTPases signal pathway as superoxide.

Discussion

In various pathophysiological situations, such as inflammation, malignancy, arterial sclerosis, tissue damage, etc., cells in the lesion are incessantly exposed to ROS. In the present study, all the cells examined, which included human tongue cancer cell line SASH1, the murine macrophage-like cell line J774.1, and hPMs, became motile after superoxide treatment, suggesting a ubiquitous role of superoxide as a stimulator of cell motility. Furthermore, the finding that the addition of Cu-Zn SOD to hPMs or J774.1 cells suppressed their motility, suggests that the automotility of those cells is largely dependent on the superoxide, which they themselves generate, i.e., an autocrine stimulation of the motility by superoxide.

Regarding the motility of cancer cells (SASH1), the autocrine mechanism was not operating, as self-produced superoxide was not detectable. However, as they respond to exogenous superoxide (HPX/XOD), it is suggested that cancer cells acquire invasiveness and metastatic ability as a consequence of enhanced motility stimulated by the superoxide generated by infiltrating inflammatory cells in a paracrine manner in vivo. The observation that NAC treatment of hPMs and J774.1 or Cu-Zn SOD transfection to SASH1 cells almost completely nullified the motility of these cells implies the essentiality of intracellular superoxide as a generator of cell motility at the basal level (intrinsic motility). This recognition of the essentiality of intracellular superoxide for cell motility is consistent with our previous observation that an inverse relationship existed between intracellular Cu-Zn SOD activity and invasiveness of tumor cells. We used a tetracycline regulation system for transient expression of Cu-Zn SOD, as it was previously reported that forced long-term expression of SOD gene brought about growth suppression of the transfectants (Liu et al., 1997). With respect to the mechanism whereby extracellular superoxide increases intracellular superoxide, penetration through cell membrane may be a possibility (Lynch and Fridovich, 1978; Gus'kova et al., 1984; Mao and Poznansky, 1992; Gomes et al., 1993), although the proof remains to be established.

To substantiate the idea that superoxide induces motility, we investigated the underlying molecular mechanism. The first issue we addressed was whether, and to what extent, the Rho family of small GTP-binding proteins was involved in the signal transduction of superoxide-induced cell movement, as these proteins are well accepted as common mediators of the cell signals for various stimuli. RhoA, Rac1, and Cdc42 were each activated by superoxide stimulation in all three cells examined. The motility of SASH1 cells was markedly suppressed by C3, DNRac1, and DNCdc42, with C3 limiting motility to basal levels in hPMs and J774.1 cells. Together, these results indicate that ROS induces cell motility via Rho family GTPase activation. Furthermore, each single GTPase may be indispensable for the cell movement induced by superoxide.

Next, we searched for the molecule that may link the superoxide signal with Rho family GTPases. It has been reported that stimulators of cell motility, such as lysophophatidic acid and insulin, activate both Rho family GTPases and PKC simultaneously (Hall, 1994; Machesky and Hall, 1996). Translocation of RhoA to membrane and RhoA-dependent phospholipase D

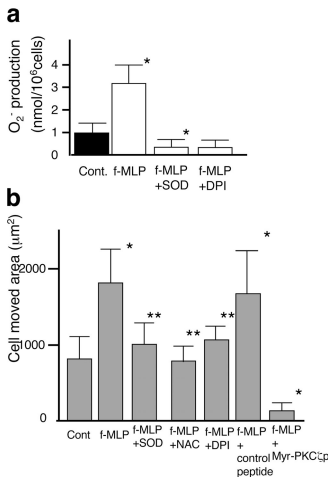

Figure 8. **Response of J774.1 cells to fMLP.** (a) Superoxide production of J774.1 cells treated with fMLP was measured by cytochrome *c* method. (b) Motility of J774.1 cells was measured by phagokinetic track assay. fMLP was added at 10 μM fMLP, SOD was added at 100 U/ml, NAC was added at 40 mM, DPI was added at 20 μM, control peptide was added at 50 μM, and myr-PKCζp was added at 50 μM. Error bars indicate SEM.

activation induced by GTPγS are reportedly blocked by calphostin C in MDCK cells (Balboa and Insel, 1995). Activation of RhoA by phosphorylating RhoGDI-1 by PKCα has been observed in human umbilical venular endothelial cells stimulated with thrombin (Mehta et al., 2001). In addition to these reports, previous evidence indicating activation of PKCs by oxidative stress (Konishi et al., 1997; Klann et al., 1998) led us to hypothesize that PKC is the linking molecule. This hypothesis was supported by the fact that calphostin C suppressed motility and activation of RhoGTPases in all three types of cells. With regard to the mechanism for activation of PKC by superoxide, the involvement of PI3-kinase in linking these molecules is conceivable because PI3-kinase has been known to activate PKCζ via PDK-1 phosphorylation in vitro (Chou et al., 1998). However, the fact that the inhibitor of PI3-kinase, LY294002, did not inhibit superoxide-induced RhoA or Cdc42 activation in our cells (unpublished data) negated this possibility. Thus, it seems likely that superoxide activates PKC either through activation of kinases other than PI3-kinase or through direct activation of PKC by superoxide, possibly by causing conformational change (Palumbo et al., 1992). Elucidation of these putative mechanisms remains a future task.

Given that PKC is involved in signaling from superoxide to all three RhoGTPases, it is highly plausible that PKC interacts with RhoGDI-1 to activate RhoGTPases, because inactive RhoA, Rac1, and Cdc42 are commonly bound to RhoGDI-1. Therefore, using SASH1, J774.1 cells, and hPMs, we examined the direct interaction between PKCs and RhoGDI-1 by IP and found that only one specific isozyme of PKCs, PKCζ, was coprecipitable with RhoGDI-1. This observation, taken collectively with the facts that treatment with DNPKCζ or inhibitory peptide of PKCζ caused suppression of motility and the activation of the GTPases, strongly supports the notion that this particular PKC isozyme is a signal transducer of superoxide.

It has been shown that peroxide activates various PKC isozymes expressed in COS cells (Konishi et al., 1997). We also found that superoxide treatment of SASH1 brought about activation of all types of PKCs expressed in the cell, as determined by their translocation to the plasma membrane. In this context, the specific binding of PKCζ to RhoGDI-1 can be rationalized by the speculation that this isozyme has higher binding affinity than other PKC isotypes to the substrate (RhoGDI-1), and not by the specific activation of PKCζ by superoxide.

It is generally accepted that for activation of RhoGTPases, their release from the RhoGDI-1 molecule is required. It was recently reported that PKCα, activated by thrombin, can phosphorylate RhoGDI-1, catalyzing the release of bound GTPases (Mehta et al., 2001). Our present results indicate that superoxide stimulates PKCζ, which in turn leads to RhoGDI-1 phosphorylation at threonine sites to liberate RhoGTPases. These results are compatible with the aforementioned study, except for the stimulant (superoxide) and signal transducer (PKCζ).

As inflammatory cells are usually attracted and activated by chemokines in the lesion, we further studied the role of superoxide in motility of J774.1 and hPMs induced by fMLP, a chemotactic peptide that is known to interact with 7-transmembrane G-coupled formyl-peptide receptors (Le et al., 2002). Our findings that fMLP treatment of these cells stimulated superoxide generation, which was suppressed by DPI, a specific inhibitor of NADPH oxidase, confirmed the notion that chemokines activate PKCζ to stimulate NADPH oxidase at plasma membrane, in turn generating superoxide (Bokoch 1995; Dang et al., 2001). On the basis of these findings, we extended our investigation to elucidate the relevance of fMLP-induced motility to superoxide generated by the cells treated with fMLP. The results that Cu-Zn SOD or DPI treatment suppressed the motility of J774.1 and hPMs support the concept of autocrine activation of chemokine-induced motility via superoxide. It was speculated that NAC should scavenge out intracellular superoxide and thereby abrogate superoxide-induced cell motility. However, when the fMLP-stimulated J774.1 cells or hPMs were pretreated with NAC, a certain magnitude of motility unexpectedly remained. The results therefore imply that fMLP interaction with chemokine receptor stimulates multiple pathways to activate cell motility. Furthermore, the fact that myr-PKCζp suppressed the motility of J774.1 cells and hPMs to basal level suggests the possibility that the other signal (as well as superoxide-relevant one) is also mediated by PKCζ. This notion, activation of PKCζ through interaction of chemokine with its receptor, is veritably compatible with the recent report that atypical PKCζ regulates stromal cell–derived factor-1 mediated migration of human CD34+ progenitor cells (Petit et al., 2005). Hence, it may be reasonable to deduce that fMLP binds its receptors to activate PKCζ to generate superoxide, which in turn stimulates the motility in an autocrine manner via the PKCζ–RhoGDI-1–RhoGTPase pathway. On the other hand, PKCζ activated by fMLP simultaneously induces motility via the common PKCζ–RhoGDI-1–RhoGTPase pathway. Accordingly, the motility induced by chemokine is considered to be at least partly dependent on superoxide.

In conclusion, we disclosed that superoxide plays a pivotal role in the motility of SASH1, J774.1, and hPMs through a novel signaling pathway of PKCζ–RhoGDI-1–RhoGTPases. Thus, these results suggest a new approach for manipulation of inflammation as well as tumor cell invasion by targeting this novel signaling pathway.

Materials and methods

Cells and cell culture

SASH1, a poorly differentiated human squamous cell carcinoma line was cultured in DME/F-12 (Invitrogen), and murine macrophage-like cell line J774.1 was cultured in RPMI (Invitrogen) supplemented with 10% FCS in humidified 5% CO_2 at 37°C. To attain the quiescent state, cells were cultured in the medium without FCS for 20 h.

Culture of peripheral blood monocytes

CD14+ monocytes were isolated from peripheral blood mononuclear cells of healthy volunteers obtained by the standard Ficoll-Paque method and separated by negative magnetic depletion using hapten-conjugated CD3, CD7, CD19, CD45RA, CD56, and anti-IgE antibodies (MACS; Miltenyi Biotec) and a magnetic cell separator (MACS) according to the manufacturer's instructions.

Superoxide and NAC treatment

Serum-starved cultures on 100-mm dishes were treated with 4 μg/ml HPX (Sigma-Aldrich) and 7×10^{-3} U/ml XOD (Sigma-Aldrich) for various incubation periods noted in each experiment. For NAC treatment, NAC

(Sigma-Aldrich) was dissolved in the medium, pH adjusted to 7.4, and the cells were treated for 1 h.

Measurement of phagokinetic tracks
A uniform carpet of gold particles was prepared as previously described (Albrecht-Buehler, 1977). In brief, sterilized coverslips were coated with 1% bovine serum albumin and were placed in 35-mm tissue culture dishes. Gold colloidal solution (184 μM $HAuCl_4$-$4H_20$ and 11.6 mM Na_2CO_3) was boiled shortly to make gold colloidal particles, and the coverslips were coated with them. 2×10^3 serum-starved cells with various pretreatments described in each experiment were seeded, attached to the coverslips, treated with or without superoxide, and 2 h later fixed by 0.1% formaldehyde. The areas cleared of gold particles were examined under microscope and quantified by image processing (KS400; Carl Zeiss MicroImaging, Inc.).

Evaluation of intracellular ROS level
Intracellular ROS level was evaluated using DHR 123 (Invitrogen) as a fluorescent probe. After cells were treated with various conditions, as indicated, 1 μl of 43.3 mM DHR was added to the cells suspended with 1 ml HBSS for 20 min, cells were washed, the generation of rhodamine 123 was monitored on a FACScan (Becton Dickinson) with excitation at 488 nm, and the emitted fluorescence was collected at 525 nm.

F-actin staining
The cells were fixed in 3% paraformaldehyde for 20 min, permeabilized with 0.2% Triton X-100 for 5 min, and stained with rhodamine-labeled phalloidin (Invitrogen) for 40 min to visualize F-actin. Fluorescence images were obtained by a confocal laser-scanning microscope system with 40× objective lens (LSM5 PASCAL; Carl Zeiss MicroImaging, Inc.).

Preparation of recombinant *Clostridium botulinum* C3 exoenzyme and ADP-ribosylation assay
Preparation of recombinant *C. botulinum* C3 exoenzyme and ADP-ribosylation assay were performed as described previously (Morii and Narumiya, 1995). The C3-expressing plasmid pET3a C3 was provided by S. Narumiya (Kyoto University Faculty of Medicine, Kyoto, Japan).

Immunodetection of RhoGDI-1–associated proteins
Cells were lysed in lysis buffer (20 mM Tris/HCl, pH 7.5, 10 mM $MgCl_2$, 1 mM pefabloc, 5 mM leupeptin, and 5 mM pepstatin) containing 1% NP-40 and were incubated with protein G–agarose beads (GE Healthcare) for 3 h to block the nonspecific binding. After centrifugation, the supernatant was incubated with anti–RhoGDI-1 antibody (Santa Cruz Biotechnology, Inc.) for 3 h, followed by the addition of protein G–agarose beads, and agitated overnight. The beads were collected, washed, and further analyzed by immunoblotting. For immunoblotting, each aliquot of the sample was eluted by RhoGDI-1 peptide, mixed in SDS sample buffer, heated, separated on SDS-PAGE, and electroblotted. Antibodies against RhoA (26C4), RhoGDI-1, and PKCζ were purchased from Santa Cruz Biotechnology, Inc. Antibodies against Rac1 and PKCα, -β, -γ, -δ, -ε, -θ, and -μ were purchased from BD Biosciences. Antibodies against Cdc42 were purchased from Upstate Biotechnology. Antibodies against phosphothreonine and phosphoserine were purchased from Zymed Laboratories and QIAGEN.

Rho family activation assay
Activity of Rho family small GTP-binding proteins was assayed by pull-down assay using each assay kit (Upstate Biotechnology) according to the manufacturer's instruction.

PKCζ activity assay
PKCζ activity from 3×10^6 cells was assayed by assessing its phosphorylation state as described previously (Xu and Clark, 1997). In brief, PKCζ in cell lysates was immunoprecipitated with the anti-PKCζ antibody, washed, mixed in assay solution (35 mM Tris, pH 7.5, 15 mM $MgCl_2$, 1 mM $MnCl_2$, 0.5 mM EGTA, 0.1 mM $CaCl_2$, 1 mM sodium orthovanadate, and 100 μM γ-[^{32}P]ATP), and incubated at 30°C for 10 min. After reactions were stopped by the addition of gel loading buffer, the samples were boiled and analyzed by SDS-PAGE followed by autoradiography.

In vitro kinase assay for phosphorylation of RhoGDI
Phosphorylation of RhoGDI-1 in vitro was performed using RhoGDI-1 immunoprecipitated from SASH1 cell lysate with RhoGDI-1 antibody. Confluent cells grown in 100-mm dishes were washed with ice-cold PBS and lysed in IP buffer containing 50 mM Tris, pH 7.4, 150 mM NaCl, 0.25 mM EDTA, pH 8.0, 1% deoxycholic acid, 1% Triton X-100, 5 mM NaF, 1 mM sodium orthovanadate, 1 mM PMSF, 5 μg/ml leupeptin, 5 μg/ml aprotinin, and 1 μg/ml pepstatin A. The cells were collected and then cleared by centrifugation at 4°C at 14,000 *g* for 10 min. The lysate was incubated with anti–RhoGDI-1 antibody for 1 h followed by the addition of protein G–Sepharose beads overnight at 4°C. The beads were collected, washed twice with ice-cold lysate buffer, washed three times with PBS, and washed once with kinase buffer (8 mM MOPS, pH 7.4, and 0.2 mM EGTA). The immunoprecipitated RhoGDI-1 was incubated with 5 ng of recombinant active PKCζ in kinase assay buffer for 10 min at 30°C followed by the addition of magnesium/ATP cocktail (Upstate Biotechnology): 4 mM $MgCl_2$ and 25 μM ATP in 1 mM MOPS, pH 7.2, 1 mM β-glycerol phosphate, 0.2 mM EGTA, 50 μM sodium orthovanadate, 50 μM dithiothreitol, and 10 μCi γ-[^{32}P]ATP (stock 1 mCi/100 μl: 3,000 Ci/mmol; PerkinElmer). The reaction was stopped by the addition of Laemmli sample buffer. The samples were electrophoresed on a 10% SDS-polyacrylamide gel, transferred to nitrocellulose membrane, and exposed to x-ray film. The blots were then subjected to Western blotting with anti–RhoGDI-1 antibody to verify that an equal amount of the protein loaded in each lane.

Subcellular fractionation
Cells were washed three times with ice-cold PBS and scraped in lysis buffer (20 mM Tris/HCl, pH 7.5, 10 mM $MgCl_2$, 1 mM pefabloc, 5 mM leupeptin, and 5 mM pepstatin). The cells were lysed by 18 passes through a 26-gauge needle on ice. Trypan blue staining of the lysate indicated >95% disruption of plasma membrane. The subcellular fractionation was performed by the method as described by Fleming et al. (1996). The lysate was first centrifuged at 500 *g* for 10 min to prepare low-speed pellet, and the supernatant was recentrifuged at 120,000 *g* for 45 min to pellet the remainder of the particulate fraction (high-speed pellet). The low-speed pellet was further purified by sucrose gradient centrifugation to obtain plasma membrane fraction. Protein concentrations were determined using BCA protein assay (Pierce Chemical Co.) according to the manufacturer's directions. Alkaline phosphodiesterase I, cytochrome *c* oxidase, and lactate dehydrogenase were used as marker enzymes for plasma membrane, mitochondria, and cytosol, respectively (Storrie and Madden, 1990). DNA and RNA were used as markers for nucleus and endoplasmic reticulum, respectively, and were detected on agarose gels by ethidium bromide staining, with or without RNase treatment. After subfractionation of the cells, plasma membrane fractions were subjected for immunoblotting to measure PKC or RhoGTPase activity.

Cu-Zn SOD plasmid
The pTA-Hyg and pET2a vectors were provided by J. Yokota (National Cancer Center Research Institute, Tokyo, Japan). cDNA for the human Cu-Zn SOD expression vector was generated by PCR using the forward primer 5′-TTTCCGTTGCAGTCCTCGGAA-3′ and the reverse primer 5′-CCTCAGACTACATCCAAGGGA-3′ with the human cDNA library as the template. The PCR fragment was ligated into the pET2a vector to generate pET2a Cu-Zn SOD vector, which expresses Cu-Zn SOD when tetracycline is omitted from the medium. SASH1 cells were first transduced with the pTA-Hyg vector, selected by hygromycin B, transfected with the pET2a Cu-Zn SOD vector, and selected by G418.

Plasmid for DNRac1 and DNCdc42
cDNA of N17Rac1 and N17Cdc42, which are DN cDNAs of Rac1 and Cdc42, were provided by Y. Takai (Osaka University, Osaka, Japan). N17Rac1 was first ligated into the pSVneo-Myc/Sra vector and then cDNA coding for Rac1N17 tagged with Myc was digested and ligated into the pIRES/neo vector, resulting in pIRES-Rac1N17-Myc/neo. N17Cdc42 was first ligated into the pFlag-CMV vector and then cDNA coding for N17Cdc42 tagged with Flag was digested and ligated into the pIRES/hyg vector, resulting in pIRES-Cdc42N17-Flag/hyg.

Plasmid for N- and C-terminal of PKCζ
cDNA coding for the N- or C-terminal of human PKCζ was generated by PCR with the human cDNA library as the template using the First strand cDNA Synthesis kit (Boeringer). To produce plasmid pRx-bsr-PKCζN that contains the N-terminal regulatory domain of human PKCζ (nucleotides 1–738), we used 5′-CCGGAATTCACCCAAGATGGAAGGGAGCGGCGGC-3′ as the forward primer and 5′-CGCGGATCCTCATAGGTCAAAGTCCTGCAGCCCAAGC-3′ as the reverse primer. PCR products were separated, sequenced, digested with EcoRI and NotI, and ligated into a pcDNA3.1/His (Invitrogen), and the fragment containing His6 was

excised by HindIII and NotI. It was inserted into a retroviral vector, pRx-bsr, supplied by H. Hamada (Sapporo Medical University, Sapporo, Japan). We used pRx-bsr-PKCζN regulatory domain expressing vector as DN (DNPKCζ), as this domain reportedly showed autoinhibitory activity (Jaken, 1996).

To produce plasmid PKCζC that contains the C-terminal catalytic domain of human PKCζ (nucleotides 739–1755), cDNA was generated by PCR using the forward primer 5′-CCGGAATTCAATCAGAGTCATCGGGC-GCGGGAGC-3′ and the reverse primer 5′-CGGGGTACCTCACACCGA-CTCCTCGGTGGACAGC-3′. The PCR product was digested with EcoRI and NotI and ligated into a pcDNA3.1/V5-His (Invitrogen), and the fragment containing (His)6 was excised by EcoRI and PmeI. The excised N-terminal PKCζ fragment was inserted into a retroviral vector, pRx-bsr, to construct PKCζC that contains the human C-terminal fragment of human PKCζ cDNA and (His)6. The plasmid of N- or C-terminal fragments of PKCζ was transfected into the ecotropic retroviral packaging cell line BOSC23 by the calcium phosphate precipitation method to obtain the retroviral supernatant. The amphotropic ψ Crip packaging cells were then infected with 2 ml of filtered retroviral supernatants of each plasmid in the presence of polybrene (Sigma-Aldrich).

Measurement of superoxide production

Phenol red–free medium was used in the assay. 10^6 cells were stimulated for 1 min with HPX/XOD, and the cells were further incubated for 1 h in the presence of 50 μM cytochrome *c*. The medium was removed and placed on ice, and the absorbance at 550 nm was immediately read by spectrophotometer with H_20 as a blank. Superoxide-specific reduction of cytochrome *c* was expressed as the difference in absorbance between cells incubated with or without SOD using an extinction coefficient of 21 mM^{-1} cm^{-1}.

Peptides

Myr-PKCζp, SIYRRGARRWRKLYRAN (positions 113–129, which is pseudo-substrate region of human PKCζ), and myr-control peptide, RLRYRNKRIWRS-AYAGR (Laudanna et al., 1998), were custom made by Sawaday Technology Co. They were solubilized immediately before use at 1 mM concentration in PBS, pH 7.2, and heated at 40°C to achieve complete solubility.

Statistical analysis

Statistical analysis of data was performed by standard techniques with the aid of the Stat View computer program for the Macintosh (Abacus Concepts). The means of values were provided with associated SEM. Statistical significance was defined as $P < 0.01$.

Online supplemental material

Fig. S1 shows a migration assay of SASH1 cells and J774.1 cells. Fig. S2 shows translocation of Rho family small GTPases to plasma membrane in SASH1 cells treated with superoxide. Fig. S3 shows the interaction of PKCζ catalytic domain with RhoGDI and that a SASH1 cell lysate without PKCζ did not phosphorylate recombinant RhoGDI-1. Fig. S4 shows activation of GTP-Rac2 by superoxide in J774.1 cells. Fig. S5 shows that superoxide stimulates RhoGTPases activity and motility of hPMs. Online supplemental material is available at http://www.jcb.org/cgi/content/full/jcb.200607019/DC1.

We thank J. Yokota, H. Hamada, and Y. Takai for providing vectors. We thank S. Narumiya (Kyoto University Faculty of Medicine, Kyoto, Japan) and T. Ishizaki (Kyoto University Faculty of Medicine) for generous gifts and helpful discussions. We also thank K.S. Litton, R. Holmes, and J. Ackerman for editorial assistance.

Submitted: 5 July 2006
Accepted: 21 February 2007

References

Albrecht-Buehler, G. 1977. The phagokinetic tracks of 3T3 cells. *Cell.* 11:395–404.

Balboa, M.A., and P.A. Insel. 1995. Nuclear phospholipase D in Madin-Darby canine kidney cells. Guanosine 5′-O-(thiotriphosphate)-stimulated activation is mediated by RhoA and is downstream of protein kinase C. *J. Biol. Chem.* 270:29843–29847.

Bokoch, G.M. 1995. Chemoattractant signaling and leukocyte activation. *Blood.* 86:1649–1660.

Chiarugi, P., M.L. Taddei, P. Cirri, D. Talini, F. Buricchi, G. Camici, G. Manao, G. Raugei, and G. Ramponi. 2000. Low molecular weight protein-tyrosine phosphatase controls the rate and the strength of NIH-3T3 cells adhesion through its phosphorylation on tyrosine 131 or 132. *J. Biol. Chem.* 275:37619–37627.

Chou, M.M., W. Hou, J. Johnson, L.K. Graham, M.H. Lee, C.S. Chen, A.C. Newton, B.S. Schaffhausen, and A. Toker. 1998. Regulation of protein kinase C zeta by PI 3-kinase and PDK-1. *Curr. Biol.* 8:1069–1077.

Chuang, T.H., B.P. Bohl, and G.M. Bokoch. 1993. Biologically active lipids are regulators of Rac GDI complexation. *J. Biol. Chem.* 268:26206–26211.

Coghlan, M.P., M.M. Chou, and C.L. Carpenter. 2000. Atypical protein kinases Cλ and -ζ associate with the GTP-binding protein Cdc42 and mediate stress fiber loss. *Mol. Cell. Biol.* 20:2880–2889.

Dang, P.M., A. Fontayne, J. Hakim, J. El Benna, and A. Perianin. 2001. Protein kinase C zeta phosphorylates a subset of selective sites of the NADPH oxidase component p47phox and participates in formyl peptide-mediated neutrophil respiratory burst. *J. Immunol.* 166:1206–1213.

Etienne-Manneville, S. 2004. Cdc42—the centre of polarity. *J. Cell Sci.* 117:1291–1300.

Fitzgerald, K.A., A.G. Bowie, B.S. Skeffington, and L.A. O'Neill. 2000. Ras, protein kinase C zeta, and I kappa B kinases 1 and 2 are downstream effectors of CD44 during the activation of NF-kappa B by hyaluronic acid fragments in T-24 carcinoma cells. *J. Immunol.* 164:2053–2063.

Fleming, I.N., C.M. Elliott, and J.H. Exton. 1996. Differential translocation of rho family GTPases by lysophosphatidic acid, endothelin-1, and platelet-derived growth factor. *J. Biol. Chem.* 271:33067–33073.

Furukawa, N., T. Shirotani, E. Araki, K. Kaneko, M. Todaka, K. Matsumoto, K. Tsuruzoe, H. Motoshima, K. Yoshizato, H. Kishikawa, and M. Shichiri. 1999. Possible involvement of atypical protein kinase C (PKC) in glucose-sensitive expression of the human insulin gene: DNA-binding activity and transcriptional activity of pancreatic and duodenal homeobox gene-1 (PDX-1) are enhanced via calphostin C-sensitive but phorbol 12-myristate 13-acetate (PMA) and Go 6976-insensitive pathway. *Endocr. J.* 46:43–58.

Gomes, L.F., I.M. Cuccovia, H. Chaimovich, D.H. Barbieri, and M.J. Politi. 1993. Permeation of superoxide anion through the bilayer of vesicles of a synthetic amphiphile. *Biochim. Biophys. Acta.* 1152:78–82.

Gus'kova, R.A., I.I. Ivanov, V.K. Kol'tover, V.V. Akhobadze, and A.B. Rubin. 1984. Permeability of bilayer lipid membranes for superoxide (O_2-.) radicals. *Biochim. Biophys. Acta.* 778:579–585.

Hall, A. 1994. Small GTP-binding protein and the regulation of the actin cytoskeleton. *Annu. Rev. Cell Biol.* 10:31–54.

Hancock, J.F., and A. Hall. 1993. A novel role for RhoGDI as an inhibitor of GAP proteins. *EMBO J.* 12:1915–1921.

Hart, M.J., X. Jiang, T. Kozasa, W. Roscoe, W.D. Singer, A.G. Gilman, P.C. Sternweis, and G. Bollag. 1998. Direct stimulation of the guanine nucleotide exchange activity of p115 RhoGEF by Galpha13. *Science.* 280:2112–2114.

Isomura, M., A. Kikuchi, N. Ohga, and Y. Takai. 1991. Regulation of binding of rhoB p20 to membranes by its specific regulatory protein, GDP dissociation inhibitor. *Oncogene.* 6:119–124.

Jaken, S. 1996. Protein kinase C isozymes and substrates. *Curr. Opin. Cell Biol.* 8:168–173.

Klann, E., E.D. Roberson, L.T. Knapp, and J.D. Sweatt. 1998. A role for superoxide in protein kinase C activation and induction of long-term potentiation. *J. Biol. Chem.* 273:4516–4522.

Kodama, A., T. Matozaki, A. Fukuhara, M. Kikyo, M. Ichihashi, and Y. Takai. 2000. Involvement of an SHP-2-Rho small G protein pathway in hepatocyte growth factor/scatter factor-induced cell scattering. *Mol. Biol. Cell.* 11:2565–2575.

Kogawa, K., H. Muramatsu, M. Tanaka, Y. Nishihori, S. Hagiwara, K. Kuribayashi, K. Nakamura, K. Koike, S. Sakamaki, and Y. Niitsu. 1999. Enhanced inhibition of experimental metastasis by the combination chemotherapy of Cu-Zn SOD and adriamycin. *Clin. Exp. Metastasis.* 17:239–244.

Konishi, H., M. Tanaka, Y. Takemura, H. Matsuzaki, Y. Ono, U. Kikkawa, and Y. Nishizuka. 1997. Activation of protein kinase C by tyrosine phosphorylation in response to H_2O_2. *Proc. Natl. Acad. Sci. USA.* 94:11233–11237.

Laudanna, C., D. Mochly-Rosen, T. Liron, G. Constantin, and E.C. Butcher. 1998. Evidence of zeta protein kinase C involvement in polymorphonuclear neutrophil integrin-dependent adhesion and chemotaxis. *J. Biol. Chem.* 273:30306–30315.

Le, Y., P.M. Murphy, and J.M. Wang. 2002. Formyl-peptide receptors revisited. *Trends Immunol.* 23:541–548.

Liu, K., S. Hsiung, M. Adlersberg, T. Sacktor, M.D. Gershon, and H. Tamir. 2000. Ca^{2+}-evoked serotonin secretion by parafollicular cells: roles in signal transduction of phosphatidylinositol 3′-kinase, and the gamma and zeta isoforms of protein kinase C. *J. Neurosci.* 20:1365–1373.

Liu, R., T.D. Oberley, and L.W. Oberley. 1997. Transfection and expression of MnSOD cDNA decreases tumor malignancy of human oral squamous carcinoma SCC-25 cells. *Hum. Gene Ther.* 8:585–595.

Lynch, R.E., and I. Fridovich. 1978. Permeation of the erythrocyte stroma by superoxide radical. *J. Biol. Chem.* 253:4697–4699.

Machesky, L., and A. Hall. 1996. Rho: a connection between membrane receptor signalling and the cytoskeleton. *Trends Cell Biol.* 6:304–310.

Mao, G.D., and M.J. Poznansky. 1992. Electron spin resonance study on the permeability of superoxide radicals in lipid bilayers and biological membranes. *FEBS Lett.* 305:233–236.

Mehta, D., A. Rahman, and A.B. Malik. 2001. Protein kinase C-alpha signals rho-guanine nucleotide dissociation inhibitor phosphorylation and rho activation and regulates the endothelial cell barrier function. *J. Biol. Chem.* 276:22614–22620.

Moolenaar, W.H., L.A. van Meeteren, and B.N. Giepmans. 2004. The ins and outs of lysophosphatidic acid signaling. *Bioessays.* 26:870–881.

Morii, N., and S. Narumiya. 1995. Preparation of native and recombinant *Clostridium botulinum* C3 ADP-ribosyltransferase and identification of Rho proteins by ADP-ribosylation. *Methods Enzymol.* 256:196–206.

Muramatsu, H., K. Kogawa, M. Tanaka, K. Okumura, Y. Nishihori, K. Koike, T. Kuga, and Y. Niitsu. 1995. Superoxide dismutase in SAS human tongue carcinoma cell line is a factor defining invasiveness and cell motility. *Cancer Res.* 55:6210–6214.

Nobes, C.D., and A. Hall. 1995. Rho, rac, and cdc42 GTPases regulate the assembly of multimolecular focal complexes associated with actin stress fibers, lamellipodia, and filopodia. *Cell.* 81:53–62.

Palumbo, E.J., J.D. Sweatt, S.J. Chen, and E. Klann. 1992. Oxidation-induced persistent activation of protein kinase C in hippocampal homogenates. *Biochem. Biophys. Res. Commun.* 187:1439–1445.

Petit, I., P. Goichberg, A. Spiegel, A. Peled, C. Brodie, R. Seger, A. Nagler, R. Alon, and T. Lapidot. 2005. Atypical PKC-zeta regulates SDF-1-mediated migration and development of human CD34+ progenitor cells. *J. Clin. Invest.* 115:168–176.

Ridley, A.J. 2001. Rho GTPases and cell migration. *J. Cell Sci.* 114:2713–2722.

Slater, S.J., J.L. Seiz, B.A. Stagliano, and C.D. Stubbs. 2001. Interaction of protein kinase C isozymes with Rho GTPases. *Biochemistry.* 40:4437–4445.

Spitaler, M., and D.A. Cantrell. 2004. Protein kinase C and beyond. *Nat. Immunol.* 5:785–790.

Sultana, C., Y. Shen, V. Rattan, C. Johnson, and V.K. Kalra. 1998. Interaction of sickle erythrocytes with endothelial cells in the presence of endothelial cell conditioned medium induces oxidant stress leading to transendothelial migration of monocytes. *Blood.* 92:3924–3935.

Storrie, B., and E.A. Madden. 1990. Isolation of subcellular organelles. *Methods Enzymol.* 182:203–225.

Tanaka, M., K. Kogawa, Y. Nishihori, K. Kuribayashi, K. Nakamura, H. Muramatsu, K. Koike, S. Sakamaki, and Y. Niitsu. 1997. Suppression of intracellular Cu-Zn SOD results in enhanced motility and metastasis of Meth A sarcoma cells. *Int. J. Cancer.* 73:187–192.

Tanaka, M., K. Kogawa, K. Nakamura, Y. Nishihori, K. Kuribayashi, S. Hagiwara, H. Muramatsu, S. Sakamaki, and Y. Niitsu. 2001. Anti-metastatic gene therapy utilizing subcutaneous inoculation of EC-SOD gene transduced autologous fibroblast suppressed lung metastasis of Meth-A cells and 3LL cells in mice. *Gene Ther.* 8:149–156.

Thelen, M. 2001. Dancing to the tune of chemokines. *Nat. Immunol.* 2:129–134.

Uberall, F., K. Hellbert, S. Kampfer, K. Maly, A. Villunger, M. Spitaler, J. Mwanjewe, G. Baier-Bitterlich, G. Baier, and H.H. Grunicke. 1999. Evidence that atypical protein kinase C-λ and atypical protein kinase C-ζ participate in Ras-mediated reorganization of the F-actin cytoskeleton. *J. Cell Biol.* 144:413–425.

Ueda, T., A. Kikuchi, N. Ohga, J. Yamamoto, and Y. Takai. 1990. Purification and characterization from bovine brain cytosol of a novel regulatory protein inhibiting the dissociation of GDP from and the subsequent binding of GTP to rhoB p20, a ras p21-like GTP-binding protein. *J. Biol. Chem.* 265:9373–9380.

Woo, C.H., M.H. Yoo, H.J. You, S.H. Cho, Y.C. Mun, C.M. Seong, and J.H. Kim. 2003. Transepithelial migration of neutrophils in response to leukotriene B4 is mediated by a reactive oxygen species-extracellular signal-regulated kinase-linked cascade. *J. Immunol.* 170:6273–6279.

Xu, J., and R.A.F. Clark. 1997. A three-dimensional collagen lattice induces protein kinase C-zeta activity: role in beta2 integrin and collagenase mRNA expression. *J. Cell Biol.* 136:473–483.

Yoshizaki, N., Y. Mogi, H. Muramatsu, K. Koike, K. Kogawa, and Y. Niitsu. 1994. Suppressive effect of recombinant human Cu, Zn-superoxide dismutase on lung metastasis of murine tumor cells. *Int. J. Cancer.* 57:287–292.